ARTICLE
Journal of Cellular Biochemistry 113:695–710 (2012)

Journal of Cellular Biochemistry

AMPK Promotes Skeletal Muscle Autophagy Through Activation of Forkhead FoxO3a and Interaction With Ulk1

Anthony MJ Sanchez,[1,2*] Alfredo Csibi,[2] Audrey Raibon,[2] Karen Cornille,[2] Stéphanie Gay,[2] Henri Bernardi,[2] and Robin Candau[1,2]

[1] *INRA, UMR866 Dynamique Musculaire et Métabolisme, 2 Place Viala, F-34060 Montpellier, France*

[2] *Université de Montpellier 1, Faculté des Sciences du Sport, 700 av du Pic Saint-Loup, F-34090 Montpellier, France*

ABSTRACT

In skeletal muscle, protein levels are determined by relative rates of protein synthesis and breakdown. The balance between synthesis and degradation of intracellular components determines the overall muscle fiber size. AMP-activated protein kinase (AMPK), a sensor of cellular energy status, was recently shown to increase myofibrillar protein degradation through the expression of MAFbx and MuRF1. In the present study, the effect of AMPK activation by AICAR on autophagy was investigated in muscle cells. Our results show that FoxO3a transcription factor activation by AMPK induces the expression of the autophagy-related proteins LC3B-II, Gabarapl1, and Beclin1 in primary mouse skeletal muscle myotubes and in the Tibialis anterior (TA) muscle. Time course studies reveal that AMPK activation by AICAR leads to a transient nuclear relocalization of FoxO3a followed by an increase of its cytosolic level. Moreover, AMPK activation leads to the inhibition of mTORC1 and its subsequent dissociation of Ulk1, Atg13, and FIP200 complex. Interestingly, we identify Ulk1 as a new interacting partner of AMPK in muscle cells and we show that Ulk1 is associated with AMPK under normal conditions and dissociates from AMPK during autophagy process. Moreover, we find that AMPK phosphorylates FoxO3a and Ulk1. In conclusion, our data show that AMPK activation stimulates autophagy in skeletal muscle cells through its effects on the transcriptional function of FoxO3a and takes part in the initiation of autophagosome formation by interacting with Ulk1. Here, we present new evidences that AMPK plays a crucial role in the fine tuning of protein expression programs that control skeletal muscle mass. J. Cell. Biochem. 113: 695–710, 2012.

KEY WORDS: AMPK; AUTOPHAGY; ULK1; ATROPHY; AICAR

The maintenance of muscle mass is controlled by a fine balance between catabolic and anabolic processes, which determines the level of muscle proteins and the diameter of muscle fibers. Skeletal muscle atrophy can be defined as a decrease in muscle fiber diameter, protein content, force production, and fatigue resistance [Jackman and Kandarian, 2004]. This process can result from a plethora of causes including immobilization, denervation, aging, and neuromuscular diseases. Moreover, muscle atrophy can be secondary to some devastating injuries or health problems such as spinal cord injury [Castro et al., 1999], cancer cachexia, sepsis, diabetes, or AIDS, and exacerbated by glucocorticoid treatment, micro-gravity, and starvation [Mitch and Goldberg, 1996; Fitts et al., 2001; Lecker et al., 2004].

AMP-activated protein kinase (AMPK) is a serine–threonine kinase that is activated upon electrically stimulated muscle contraction [Vavvas et al., 1997; Derave et al., 2000], exercise [Wojtaszewski et al., 2000], and by AICAR treatment [Salt et al., 2000]. In response to energy depletion, AMPK activation promotes

Abbreviations: AICAR, 5-aminoimidazole-4-carboxamide-1-ß-D-ribofuranoside; AMPK, 5′ adenosine monophosphate-activated protein kinase; DM, differentiation medium; DMEM, Dulbecco's modified Eagle's medium; FCS, fetal calf serum; FIP200, focal adhesion kinase (FAK) family interacting protein of 200 kDa; IGF-1, insulin like growth factor 1; MAFbx, Atrogin-1/muscle atrophy F-box; MyHC, myosin heavy chain; mTOR, mammalian target of rapamycin; MuRF1, Muscle RING Finger 1; PARP, poly(ADP-ribose) Polymerase; PI3K, phosphatidylinositol-3-phosphate kinase; Rheb, Ras homologous enriched in brain; rpS6, ribosomal protein S6; S6K1, ribosomal S6 kinase 1; TSC2, Tuberous Sclerosis Complex 2; Ulk1, Unc51-like kinase 1; 4E-BP1, eIF4E-binding protein 1.

Conflicts of interest: None.

Henri Bernardi and Robin Candau contributed equally to this work.

Alfredo Csibi's present address is Harvard Medical School, Boston.

*Correspondence to: Anthony MJ Sanchez, INRA, UMR866 Dynamique Musculaire et Métabolisme, Faculté des Sciences du Sport, Université Montpellier 1, 2 place Viala, F-34060 Montpellier, France.
E-mail: anthony.mj.sanchez@hotmail.fr

Received 28 September 2011; Accepted 29 September 2011 • DOI 10.1002/jcb.23399 •

Published online 17 October 2011 in Wiley Online Library (wileyonlinelibrary.com).

metabolic changes to maintain cell proliferation and survival [Hardie, 2007]. AMPK is thought to act as a negative regulator of protein synthesis and to modulate muscle mass [Nader et al., 2002]. Activation of AMPK inhibits the mammalian target of rapamycin complex 1 (mTORC1), a multiprotein complex composed of mTOR, raptor, mLST8, and PRAS40 [Wullschleger et al., 2006; Ma and Blenis, 2009] which controls skeletal muscle mass [Bodine et al., 2001b; Rommel et al., 2001]. Moreover, a recent work associated the activation of AMPK with increased myofibrillar proteolysis in muscle cells [Nakashima et al., 2008]. Nevertheless, while it is well known that the molecular mechanisms through AMPK contribute to decreased protein synthesis rates, the direct implication of AMPK in mediating signaling pathways involved in skeletal muscle atrophy remains unclear.

Protein degradation is essentially mediated by two conserved pathways: The ATP-dependent ubiquitin-proteasome system and the autophagy-lysosomal pathway. The first one involves a cascade of enzymatic reactions that label substrate proteins with ubiquitin chains for degradation by the 26S proteasome. This system involves the activity of E3 ubiquitin ligases, which confer substrate specificity for ubiquitination. Two major E3 ligases have been described to be essential for muscle atrophy, atrogin-1/MAFbx (Muscle Atrophy F-box) and MuRF1 (Muscle RING Finger 1) [Bodine et al., 2001a; Gomes et al., 2001]. The second pathway, autophagy-lysosomal-dependent degradation of cytoplasmic constituents, is an important mechanism for maintaining cell metabolism and protein turnover. It involves the initial sequestration of substrates into the vacuolar system and their hydrolysis by lysosomal hydrolases [Codogno and Meijer, 2005]. Autophagy-specific gene proteins (Atgs) are essential mediators of autophagy, by controlling the formation of the autophagosome. These proteins are very abundant in skeletal muscle [Mizushima et al., 1998]. Autophagy sequestration under starvation conditions requires the conjugation of one of these Atgs, the microtubule-associated protein light chain 3 (LC3) with the phospholipids of the vacuolar membrane [Kabeya et al., 2000]. Evidence for the activation of autophagy during muscle wasting was demonstrated by the accumulation of autophagosomes in muscles of fasted transgenic GFP-LC3 mice [Mizushima et al., 2004]. Recently, collaborative studies from two groups showed that, during starvation-induced atrophy, the forkhead FoxO3a regulates the transcription of several Atgs, including LC3B, Gabarapl1, and Beclin1 [Mammucari et al., 2007; Zhao et al., 2007]. Besides its role in regulating the Atg genes, FoxO3a controls the transcription of the E3 ligases MAFbx and MuRF1 [Kamei et al., 2004; Sandri et al., 2004]. Akt phosphorylates FoxO3a on residues Thr32 and Ser253 leading to its inhibition by cytosolic retention via 14-3-3 binding [Brunet et al., 1999]. In contrast, phosphorylation of FoxO3a on residues Ser413/588 by AMPK induces its activation [Greer et al., 2007], and the AMPK-mediated phosphorylation of FoxO3a has been associated with myofibrillar proteolysis in vitro by a mechanism that seems to implicate the activity of E3 ligases [Nakashima and Yakabe, 2007]. However, whether the activation of FoxO3a by AMPK in skeletal muscle leads to activation of autophagy remains to be determined. This work addresses the potential role of AMPK in the control of skeletal muscle atrophy through FoxO3a and attempts to identify new AMPK targets involved in post-translational regulation of the autophagy pathway.

MATERIALS AND METHODS

REAGENTS

The AMP adenosine analog AICAR, insulin, and the lysosomal inhibitor Bafilomycin A1 were purchased from Sigma. Rapamycin was a kind gift from A. Sotiropoulos (Institut Cochin, Inserm U567, Paris, France). Torin1 inhibitor of mTOR was obtained from Whitehead Institute for Biomedical Research, Cambridge, MA. Preliminary experiments using 200 nM Bafilomycin A1 indicated that it has no significant effect on C2C12 and satellite cells morphology or viability.

CELL CULTURES AND TRANSFECTIONS

The mouse skeletal muscle cell line C2C12 was cultured in 36-mm dishes and grown in DMEM supplemented with 20% of fetal bovine serum and antibiotics. Myoblast fusion and differentiation was induced in subconfluent cells by replacing the medium with DMEM supplemented with 2% horse serum. Primary cultures were prepared from male mice from our own breeding stocks. All animals were treated in accordance with institutional and national guidelines. Briefly, mice satellite cells were isolated from the whole muscles of the paw. Cells were plated at a density of 2×10^4 cell/cm^2 on Matrigel-coated Petri dishes (BD Biosciences) in 80% Ham's-F10 medium containing glutamine, penicillin, and amphotericin B (Invitrogen), supplemented with 20% horse serum. After 2 days, cells were washed with Ham's-F10 and placed in complete medium supplemented with 5 ng/ml basic fibroblast growth factor. Differentiation was induced in subconfluent cells by removing the basic fibroblast growth factor. C2C12 myoblasts and primary cultures of satellite cells were transfected with 2 μg of total plasmid using Turbofect (Fermentas). Bright-field images of myotubes were randomly taken and analyzed by the Axiovision 4.4 software (Zeiss). Perfect Image version 5.5 software (Claravision, France) was used to measure diameters of at least 280 myotubes in a region where myonuclei were absent and the diameter was constant.

STARVATION

In cellulo, cells were washed three times with PBS and incubated with 1 ml modified PBS (100 mM NaCl, 5 mM KCl, 1.5 mM $MgSO_4$, 50 mM $NaHCO_3$, 1 mM NaH_2PO_4, 2 mM $CaCl_2$) without serum at 37°C during the indicated times. In vivo, animals had no access to food, but did have free access to water.

PLASMID CONSTRUCTS AND SITE-SPECIFIC MUTAGENESIS OF FoxO3a AND AMPK

Reporter plasmid pRL-HCV-FL and the pcX-cMyc Ulk1 plasmid were provided by J. Blenis (Harvard Medical School, Boston, USA), the FoxO3a human cDNA was described by Anderson et al. [1998]. The LC3 promoter (pGFP-LC3) was obtained from Yoshimori (National Institute for Basic Biology, Okazaki, Japan [Kabeya et al., 2000]. The cDNAs encoding AMPK subunits were provided by D. Carling (Imperial College, London, England) [Woods et al., 2000].

MUSCLE ELECTROTRANSFER

In vivo transfection experiments were carried out on 8-week-old C57BL/6 mice. Mice were first anaesthetized with isoflurane (0.75–1% in oxygen) and received a single injection of 0.4 U of bovine hyaluronidase (Sigma) in 25 μl 0.9% NaCl into the Tibialis anterior (TA) muscle. After 2 h, a total of 15 μg of plasmid DNA in 0.9% NaCl was injected into each TA under conditions of ketamine (100 μg per gram body weight) and xylazine (10 μg/g) anaesthesia. pEGFP was used as a control. An electrical field was then applied to muscle with caliper rule electrodes coated with ultrasound transmission gel (Aquasonic 100, Parker) and placed on each side of the leg. Six square-wave 130 V/cm pulses, lasting 60 ms each with a 100 ms interval, were then applied with a BTX electrocell manipulator. Fourteen days after electrotransfer, mice were killed by cervical dislocation and muscles were collected. Hind limb muscles from each animal were immediately removed and frozen in liquid nitrogen before storage at −80°C.

FLUORESCENCE MICROSCOPY AND QUANTITATIVE IMAGING

Cells were cultured on coverslips and fixed for 30 min at room temperature with 2% paraformaldehyde in PBS and then permeabilized with 0.25% Triton X-100 in PBS for 15 min at room temperature. Cells were rinsed in PBS containing Hoechst, mounted in Vectashield, viewed, and photographed as described below. Finally, the cells were observed using an inverted IX71 microscope system (Olympus, Tokyo, Japan). For EGFP-LC3 analysis, cells presenting a mostly diffuse distribution of EGFP-LC3 in the cytoplasm and nucleus were considered non-autophagic, whereas cells with more than five obvious intense punctate EGFP-LC3 aggregates with little or no nuclear localization were defined as autophagic.

IMMUNOPRECIPITATION

Muscle cells were rinsed two times in cold PBS and lysed in IP buffer [50 mM Tris pH 7.4, 150 mM NaCl, 1 mM EGTA, 0.5% NP40, 0.5 mM Na-orthovanadate, 50 mM NaF, 80μM β-glycerophosphate, 10 mM Na-pyrophosphate, 5% glycerol, and protease inhibitor mixture (Sigma)]. Cellular debris was removed by centrifugation at 10,000*g* for 10 min at 4°C. 400 μg of lysates were precleaned for 20 min with protein G-agarose (Bio Basics) and incubated with specific antibodies overnight at 4°C. After incubation, protein G beads were used for precipitation for 1 h at 4°C. The beads were then washed with IP buffer four times before being loaded onto SDS-polyacrylamide gel.

IMMUNOBLOTS AND ANTIBODIES

Proteins were loaded onto 7 and 15% SDS-polyacrylamide gels before electrophoretic transfer onto a nitrocellulose membrane (Biorad). Analyses of the mobilities of differently phosphorylated forms of 4-EBP1, and phosphorylated ribosomal S6 kinase 1 (S6K1) were made as described by Beugnet et al. [2003] After electrophoretic transfer, membranes were blocked with 50 mM Tris- HCl, pH 7.4, 150 mM NaCl, and 0.1% Tween 20 containing 5% skimmed milk and incubated overnight at 4°C with primary antibodies: Anti-myc (9E10), anti-α-tubulin (DM1A), anti-myosin heavy chain (My32), anti-Atg5 and anti-Atg13 (Sigma), ERK1/2 (Tyr204), anti-Ulk1, anti-raptor, anti-S6K1 (C-18), anti-Hdac2 and anti-Cdk4 (Santa Cruz Biotechnology), anti-Phospho-AMPK (Thr172), anti-AMPK, anti-FoxO3a, anti-Phospho-Ulk1 (Ser-467), anti-Phospho-Akt (Ser-473), anti-Akt, anti-Phospho-mTOR (Ser-2448), anti-mTOR, anti-4-EPB1, and anti-Phospho-S6 (Ser-265/236) (Cell Signaling), anti-Beclin1 (nanoTools), anti-Gabarapl1 (Proteintech Group), anti-FIP200 and anti-LC3 (Jackson), anti-GFP (Roche), and MAFbx and MuRF1 (ECM Biosciences). Nitrocellulose membranes were washed three times for 15 min with PBS-T (0.1% Tween 20) and incubated for 1 h with a peroxidase conjugated secondary antibody (Sigma). Immunoblots were revealed by using an ECL kit (Amersham Biosciences) according to the manufacturer's instructions.

NUCLEAR/CYTOSOLIC ISOLATION

The cells were washed twice with ice-cold phosphate-buffered saline and then scraped from plates in 100 μl of ice-cold lysis buffer [20 mM HEPES, pH 7.4, 10 mM NaCl, 1.5 mM $MgCl_2$, 20% glycerol, 0.1% Triton X-100, 1 mM dithiothreitol, and protease inhibitor mixture (Sigma)] according to methods adapted from Williamson et al. [2009]. The cell lysate was centrifuged at 1,000 rpm for 1 min at 4°C. The supernatant contained the cytosolic fraction. The nuclear pellet was resuspended in 50 μl of lysis buffer and 8.3 μl of 5 M NaCl was added to lyse the nuclei. This mixture was rotated at 4°C for 1 h and then centrifuged at 15,000 rpm for 15 min at 4°C. The supernatant contained the soluble nuclear fraction and the pellet was resuspended in 30 μl of lysis buffer. An equal volume of 5× SDS-PAGE loading buffer was added to each fraction. The purity of isolated fractions was verified by western analysis for Hdac2 as a nuclear indicator and α-tubulin as a cytosolic indicator.

BICISTRONIC LUCIFERASE ASSAY

Primary culture cells were transfected with pRL-HCV-FL reporter plasmid [Csibi et al., 2010]. Forty-eight hours post differentiation, cells were harvested, and the luciferase activity was measured using a Dual-Luciferase Reporter Assay System STOP and GLO kit (Promega) according to the manufacturer's instructions. Differences in the ratio of Renilla to Firefly luciferase signals were analyzed for statistical significance by one-way ANOVA with Tukey's honestly post-hoc test.

STATISTICS

Densitometry analysis of immunoblots from minimum three independent experiments was performed using Image J software. The statistical analyses were performed using GraphPad prism software (release 4, La Jolla, USA). All data are expressed as the mean ± SEM. Data were evaluated by one-way analysis of variance followed by Tukey's honestly post-hoc test. Significance was declared when $P < 0.05$.

RESULTS

AICAR TREATMENT INDUCES AUTOPHAGY IN C2C12 CELLS AND PRIMARY MOUSE SKELETAL MUSCLE MYOTUBES

Upon autophagy induction, the cytosolic autophagosome-associated protein LC3 is recruited to the membrane of nascent autophagosomes and controls their expansion [Xie et al., 2008]. Mouse C2C12 cell line

myoblasts were transfected with a plasmid coding for LC3 fused with enhanced green fluorescent protein at its N-terminus (EGFP–LC3). To test whether AICAR treatment leads to autophagosome formation, EGFP-LC3 fluorescence was localized. In complete cell culture medium containing glucose, amino acids, and serum, EGFP-LC3 fluorescence was largely diffused throughout the cytoplasm with few dots denoting basal autophagosome formation. The number of EGFP-LC3 dots rapidly increased within exposure to the mTOR inhibitor Torin1, or amino acids and serum removal (Fig. 1A), conditions that are known to stimulate autophagy in mouse embryonic fibroblasts [Meijer and Codogno, 2004; Thoreen et al., 2009]. In C2C12 myoblasts, AMPK activation by incubating myoblasts with AICAR induced the appearance of a large number of EGFP-LC3-labeled cytoplasmic vesicles consistent with the stimulation of autophagosome formation (Fig. 1A).

To ensure that punctate fluorescence detected in drug-treated myoblasts was due to modulation of autophagy, we next monitored LC3 processing and degradation. Recruitment of LC3 to nascent autophagosomes involves its proteolytic cleavage and lipidation [Yang et al., 2005]. When autophagosomes fuse with lysosomes, LC3II is cleaved by lysosomal hydrolases and the produced LC3II moiety is degraded faster than the more stable EGFP (Free-GFP) moiety, leading to transient accumulation of EGFP. The EGFP-LC3II and Free-GFP proteins can therefore be considered as characteristic proteolytic intermediates in autophagy. We showed that AICAR induces phosphorylation of AMPK and we recorded an accumulation of Free-GFP (Fig. 1B). It is noticeable that Torin1 and starvation induce a similar effect. Interestingly, we found that Rapamycin induces an increase in the number of punctuate GFP cell number but we did not report an accumulation of Free-GFP.

Autophagy is a dynamic process and the criteria we used to demonstrate autophagy, including LC3 dot formation, LC3 form conversion, and accumulation of free-GFP, reflected only the steady-state feature of autophagy. To address the question of whether our treatments on C2C12 myoblasts increased autophagosome formation or decreased autophagy degradation, we used autophagy flux assay with Bafilomycin A1. This compound inhibits the vacuolar H+ ATPase and prevents fusion between autophagosome and lysosome, leading to inhibition of LC3B-II degradation. Using this assay, we tested the effects of AICAR, Torin1, Rapamycin, and starvation and the results are shown in Figure 1C. All the treatments, including Rapamycin, increased endogenous LC3B-II levels significantly. It is noteworthy that in the presence of Bafilomycin A1, LC3B-II levels are further increased, indicating that endogenous LC3B-II is degraded by lysosomal hydrolases after formation of autolysosomes. The levels of LC3B-II accumulation in the presence of Bafilomycin A1 following autophagy activation are in the range of results previously described in C2C12 cells [Tanida et al., 2006]. Taken together these results demonstrate enhanced autophagosome formation by AICAR treatment.

To extend the results concerning the effects of AICAR treatment on the activation of autophagy pathway in proliferating C2C12 myoblasts, we analyzed this process in differentiated satellite cells. Transfection of the EGF-LC3 vector followed by AICAR treatment in primary myotubes also showed a strong increase in the number of cells displaying punctate fluorescent staining per total GFP-LC3-positive cells (Fig. 1D), an accumulation of Free-GFP, compared to control cells (Fig. 1E) and an increase in endogenous LC3B-II levels in the presence of Bafilomycin A1 (Fig. 1F). These data indicate that autophagosome formation was increased by AICAR treatment in differentiated satellite cells. Similar results were found in C2C12 myotubes (data not shown).

AICAR TREATMENT DECREASES PROTEIN TRANSLATION AND INCREASES MAFbx AND MuRF1 PROTEIN LEVELS IN PRIMARY MOUSE SKELETAL MUSCLE MYOTUBES

Since the autophagy process is associated with a decrease in protein synthesis in various cells, we examined the effects of AMPK activation on mouse primary muscle cells during terminal muscle differentiation and on C2C12 myotubes. On satellite cells, AMPK activation by AICAR leads to a decrease in myotube diameter and, interestingly, myotubes showed an enhanced atrophic pattern, characterized by a dramatic decrease in their mean diameter size

Fig. 1. AMPK activation by AICAR induces autophagy in C2C12 myoblasts and primary myotubes. A: C2C12 myoblasts were transfected with a GFP-tagged LC3 plasmid and treated in proliferative state with 1 mM AICAR for 6 h, 250 nM Torin1 for 3 h, or 50 nM Rapamycin for 3 h. Cells were starved by removal of growth medium, amino acids, and glucose and incubated in modified PBS for 3 h. Myoblasts were stained with Hoechst 33258 to visualize the nuclei. Images of representative fields were obtained by fluorescence microscopy (scale bar: 100 μm). Quantification of the percentage of cells with punctate GFP-LC3 fluorescence per total GFP-LC3-positive cells. Data represent mean ± SEM calculated from triplicates of 100 transfected cells. $^{*}P < 0.01$ compared to control. B: Total lysates from cells treated with 1 mM AICAR for 6 h, 250 nM Torin1 for 3 h, or 50 nM Rapamycin for 3 h or from 3 h-starved cells were analyzed by immunoblotting using the indicated antibodies. Cdk4 was used as a loading control. Quantification of the free GFP levels for each sample of experiments. Data displayed represent the mean and SEM of four independent experiments. $^{*}P < 0.01$ compared to control. C: C2C12 myoblasts were cultured in proliferation medium for 3 days and treated with 1 mM AICAR for 3 h, 250 nM Torin1 for 3 h, or 50 nM Rapamycin for 3 h or starved for 3 h, in the presence or absence of lysosomal inhibitor Bafilomycin A1 (100 nM). Negative control cells (EtOH) were treated with the solvent ethanol. Immunoblotting was performed to detect endogenous LC3B-II accumulation. Phospho-rps6 was used as a control of Torin1, Rapamycin, and starvation efficiency and Cdk4 was used as a loading control. Ratio of the transient accumulation of the faster running lipidated version (*LC3B-II*) to the native LC3B (*LC3B-I*) protein. Data displayed represent the mean and SEM of four independent experiments. $^{*}P < 0.01$ compared to control. $\$P < 0.01$ compared control + Bafilomycin A1. D: Mouse primary cultured satellite cells were transfected with expression vector encoding GFP-tagged LC3. Twenty four hours post transfection cells were induced to differentiate. Cells were cultured in differentiation medium for 3 days and treated with 1 mM AICAR for an additional 12 h. Images of representative fields were obtained by fluorescence microscopy (scale bar: 100 μm). Quantification of the percentage of cells with punctate GFP-LC3 fluorescence per total GFP-LC3-positive cells. Data represent mean ± SEM calculated from triplicates of 100 transfected cells each. $^{*}P < 0.01$. E: Total lysates from cells treated with 1 mM AICAR for 12 h were analyzed by immunoblotting using the indicated antibodies and phospho-specific antibodies. Cdk4 was used as a loading control. Quantification of the free GFP levels for each sample of experiments. Data displayed represent the mean and SEM of four independent experiments. $^{*}P < 0.01$ compared to control. F: Primary cultures of the mouse satellite cells were differentiated for 3 days and treated with 1 mM AICAR for an additional 12 h in the presence or absence of 200 nM Bafilomycin A1. Immunoblotting was performed to detect endogenous LC3B-II accumulation and others FoxO3a-dependent Atgs levels. Cdk4 was used as a loading control. Ratio of the transient accumulation of the faster running lipidated protein (*LC3B-II*) to the native LC3B (*LC3B-I*) protein compared with control untreated cells. Data displayed represent the mean and SEM of four independent experiments. $^{*}P < 0.01$ compared to control. $\$P < 0.01$ compared control + Bafilomycin A1.

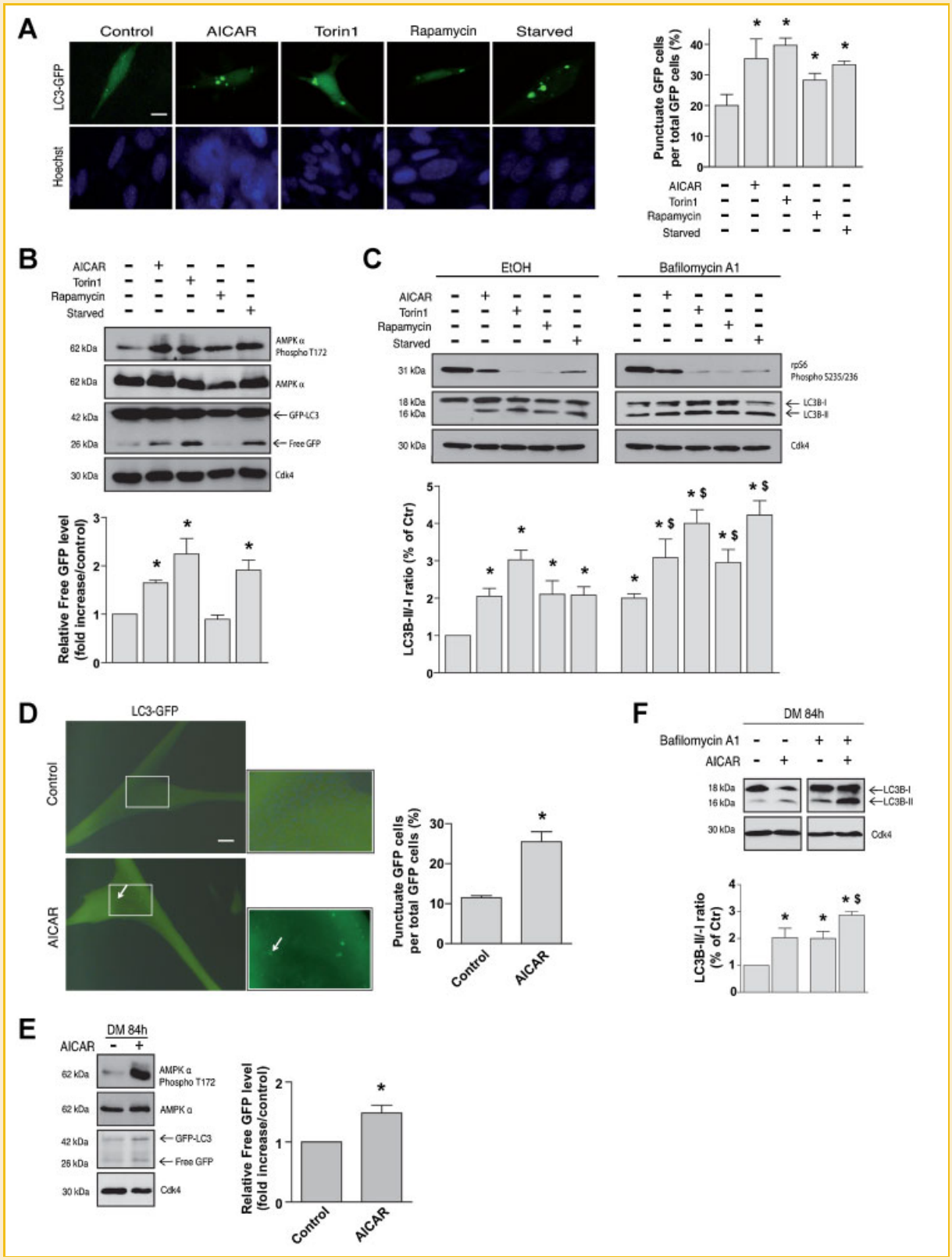
A
Control
AICAR
Torin1
Rapamycin
Starved
LC3-GFP
Hoechst
Punctuate GFP cells per total GFP cells (%)
AICAR
Torin1
Rapamycin
Starved
B
AICAR
Torin1
Rapamycin
Starved
62 kDa
AMPK α Phospho T172
62 kDa
AMPK α
42 kDa
GFP-LC3
26 kDa
Free GFP
30 kDa
Cdk4
Relative Free GFP level (fold increase/control)
C
EtOH
Bafilomycin A1
AICAR
Torin1
Rapamycin
Starved
31 kDa
rpS6 Phospho 5235/236
18 kDa
16 kDa
LC3B-I
LC3B-II
30 kDa
Cdk4
LC3B-II/-I ratio (% of Ctr)
D
LC3-GFP
Control
AICAR
Punctuate GFP cells per total GFP cells (%)
Control
AICAR
E
DM 84h
AICAR
62 kDa
AMPK α Phospho T172
62 kDa
AMPK α
42 kDa
GFP-LC3
26 kDa
Free GFP
30 kDa
Cdk4
Relative Free GFP level (fold increase/control)
Control
AICAR
F
DM 84h
Bafilomycin A1
AICAR
18 kDa
16 kDa
LC3B-I
LC3B-II
30 kDa
Cdk4
LC3B-II/-I ratio (% of Ctr)

Fig. 1.

(Fig. 2A,B). Among the myofibrillar proteins, the myosin heavy chain (MyHC) is a preferred target of multiple pro-cachectic factors inducing muscle wasting in cellulo and in vivo models [Yang et al., 2005]. This prompted us to determine whether the decrease in myotube diameter was associated with a loss of this protein. As described in Figure 2C, we observed a decrease in MyHC protein level after AICAR treatment.

Then, we examined the components of the Akt/mTORC1 pathway known to play a prominent role in muscle hypertrophy. In agreement with the results of Inoki et al. [2003] and Romanello et al. [2010], we found that AICAR treatment induces a decrease in the activity of the mTORC1 signaling including hypophosphorylation of mTOR, S6K1, and 4E-BP1, without any change in Akt phosphorylation on Ser473 and in ERK1/2 phosphorylation on Tyr204 (Fig. 2C). In addition, we assessed the phosphorylation of the direct target of S6K1, the ribosomal protein S6 (rpS6). As expected, AMPK activation by AICAR showed a decreased phosphorylation of rpS6 on Ser235/236, compared to control cells (Fig. 2C). Similar results were obtained for C2C12 myotubes (data not shown).

These results suggest that the translational machinery was less functional after AICAR treatment. To test this hypothesis, cells were transfected with a bicistronic reporter plasmid in which expression of Renilla is cap-dependent and expression of Firefly is dependent on internal ribosome entry (Fig. 2D). Differentiated transfected myotubes were treated with AICAR or stimulated with insulin as positive control, or pre-incubated with AICAR or Rapamycin and treated with insulin. Luciferase activities were measured by a dual-luciferase assay, and the renilla/firefly luciferase light-unit ratio was calculated. As expected, we found that AMPK activation by incubating myotubes with AICAR decreased the cap-dependent translation and completely inhibited the insulin-induced activation of translation as observed with Rapamycin (Fig. 2D).

The E3 ligases, MAFbx and MuRF1 are highly upregulated in many types of muscle atrophy models for protein ubiquitination and degradation [Bodine et al., 2001a; Jagoe and Goldberg, 2001]. In C2C12 myotubes, Nakashima and Yakabe [2007] reported that AMPK signaling leads to an increase in mRNA expression of MAFbx and MuRF1. Here, we analyzed the expression levels of these proteins during AMPK-induced atrophy in mouse primary muscle myotubes. Differentiated cells were treated with AICAR and lysates were analyzed by immunoblotting with the adequate antibodies. Fig. 2E shows a strong increase in MAFbx and MuRF1 protein levels after AICAR treatment. Moreover, the accumulation of ubiquitin proteins reflects an increase of the ubiquitination activity in the AICAR treated myotubes (Fig. 2E).

FoxO3a-MEDIATED AUTOPHAGY-RELATED PROTEINS ARE INDUCED BY AMPK ACTIVATION IN PRIMARY MOUSE SKELETAL MUSCLE MYOTUBES AND IN VIVO

We found here that AMPK activation by AICAR induces autophagy process in primary mouse skeletal muscle myotubes and increases MAFbx and MuRF1 protein levels. These E3 ligases being transcriptionally regulated by FoxO3a, we analyzed the expression of this factor. Figure 3A shows a strong increase of FoxO3a protein level in presence of AICAR. To investigate the implication of FoxO3a in AMPK-induced autophagy, we evaluated by immunoblotting in the presence and absence of Bafilomycin A1, the protein levels of Atgs known to be regulated by FoxO3a, in satellite cells after AICAR treatment. Figure 3B indicates that the levels of LC3B-II and Gabarapl1 are increased by Bafilomycin A1 treatment in AICAR-treated cells. In contrast, Bafilomycin A1 treatment did not significantly increase Beclin1 level, suggesting that this protein is probably not degraded by the lysosomal pathway. In accordance with our results, Zhao et al. [2007] have also reported a weak and inconsistent increase (+25%) of this protein expression following FoxO3a overexpression in myotubes.

To further address the major role of FoxO3a in mediating autophagy signaling induced by AMPK and to confirm the specificity of AICAR on AMPK, we used short hairpin RNA directed against FoxO3a (shRNA FoxO3a) and a dominant negative form of AMPK (AMPK d.n.). FoxO3a silenced cells and AMPK d.n. cells treated with AICAR exhibited an important decrease of Beclin1 accumulation, compared to the control treated cells (Fig. 3C). Autophagy flux assay performed with Gabarapl1 in presence of Bafilomycin A1, showed that, compared to control cells treated with AICAR, Gabarapl1 protein levels are significantly decreased in FoxO3a silenced satellite cells and AMPK d.n. transfected satellite cells (Fig. 3D). It is noteworthy that expression of AMPK d.n. or depletion of FoxO3a did not completely block the stimulation of LC3 lipidation upon addition of AICAR (Fig. 3C). We estimated the residual AMPK activity by immunoblot with an antibody directed against the phosphorylated AMPK (AMPK α Phospho T172). Results illustrated in Figure 3C show a residual activity of AMPK. In the same way, we measured by quantitative RT-PCR the expression of FoxO3a RNA in FoxO3a silenced cells and we found an 80% inhibition of expression (data not shown), indicating a residual expression of FoxO3a in silenced cells. Residual activity of AMPK in AMPK d.n. cells and residual expression of FoxO3a in FoxO3a-silenced cells can explain the persistence of LC3B-II expression. Nevertheless, these results confirm the major role of FoxO3a in mediating autophagy signaling induced by AMPK.

Interestingly, we found a dramatic decrease of FoxO3a protein level after transfection of the dominant negative form of AMPK suggesting the implication of AMPK in FoxO3a protein translation or stability (Fig. 3C).

To extend to a more physiological model, we electroporated expression vectors encoding constitutive active forms of AMPK (AMPK c.a.) and FoxO3a (FoxO3a c.a.) under the control of the CMV promoter into the TA muscle. Figure 3E shows that AMPK and FoxO3a overexpression like starvation, lead to an increase of the autophagy proteins LC3B-II, Gabarapl1, and Beclin1 expression.

AMPK DIRECTLY REGULATES FoxO3a SUBCELLULAR LOCALIZATION

The following experiments were conducted in C2C12 myotubes since we were not able to collect enough material for nuclear protein extraction from satellite cells. To further clarify the mode of regulation of FoxO3a by AMPK, we first determine the effects of AICAR treatment on FoxO3a localization by immunoblot. A time course experiment was performed and localization of FoxO3a was

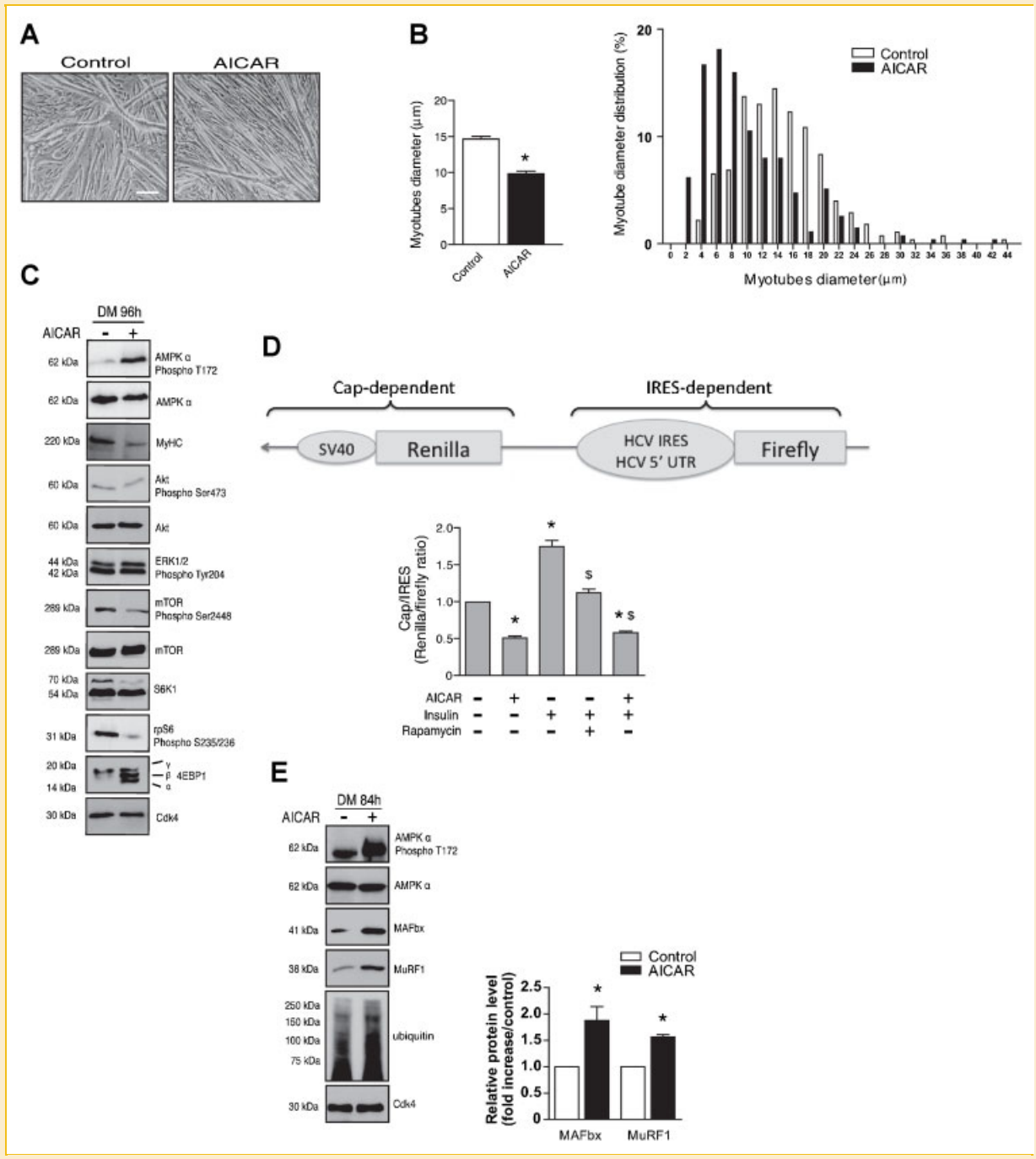

Fig. 2. AMPK activation by AICAR inhibits protein translation and increases atrophy related E3 ligases expression in primary myotubes. A: Effects of AICAR treatment on myotube size. Primary cultures of the mouse satellite cells were differentiated for 3 days and treated with 1 mM AICAR for an additional 24 h. Bright-field images of differentiated myotubes are shown. Scale bar: 20 μm. B: Mean myotube diameter and myotube diameter distribution from differentiated mouse primary cultured satellite cells treated with 1 mM AICAR. Data represent the average ± SEM for three experiments. A minimum of 280 myotubes for each condition was analyzed. $^{*}P < 0.01$ compared to control. C: Total lysates of experiments described in (A) were analyzed by immunoblotting using the indicated antibodies and phospho-specific antibodies. Cdk4 was used as a loading control. D: Activation of AMPK by AICAR modulates cap-dependent translation. Mouse primary cultured satellite cells were transfected with the bicistronic reporter vector. Twenty-four hour post transfection cells were grown for an additional 24 h in 20% serum (control), treated with 1 mM AICAR, stimulated with 100 nM insulin or pretreated for 1 h with 20 nM Rapamycin or 1 mM AICAR, and stimulated with 100 nM insulin for an additional 1 h. Luciferase activities were measured by a dual-luciferase assay. The ratio of Renilla (Cap-dependent) to Firefly (IRES-dependent) luciferase activity was calculated. Data are presented as the mean ± SEM from three independent experiments carried out in duplicate, $^{*}P < 0.05$ compared to control; $\$P < 0.05$ compared to insulin. E: Primary cultures of the mouse satellite cells were differentiated for 3 days and treated with 1 mM AICAR for an additional 12 h in the same medium. Total lysates were analyzed by immunoblotting using the indicated antibodies and phospho-specific antibodies. Tubulin was used as a loading control. Quantification of Atrogin1/MAFbx and MuRF1 expression levels in control and AICAR-treated myotubes. Data displayed represent the mean and SEM of three independent experiments. $^{*}P < 0.01$ compared to control.

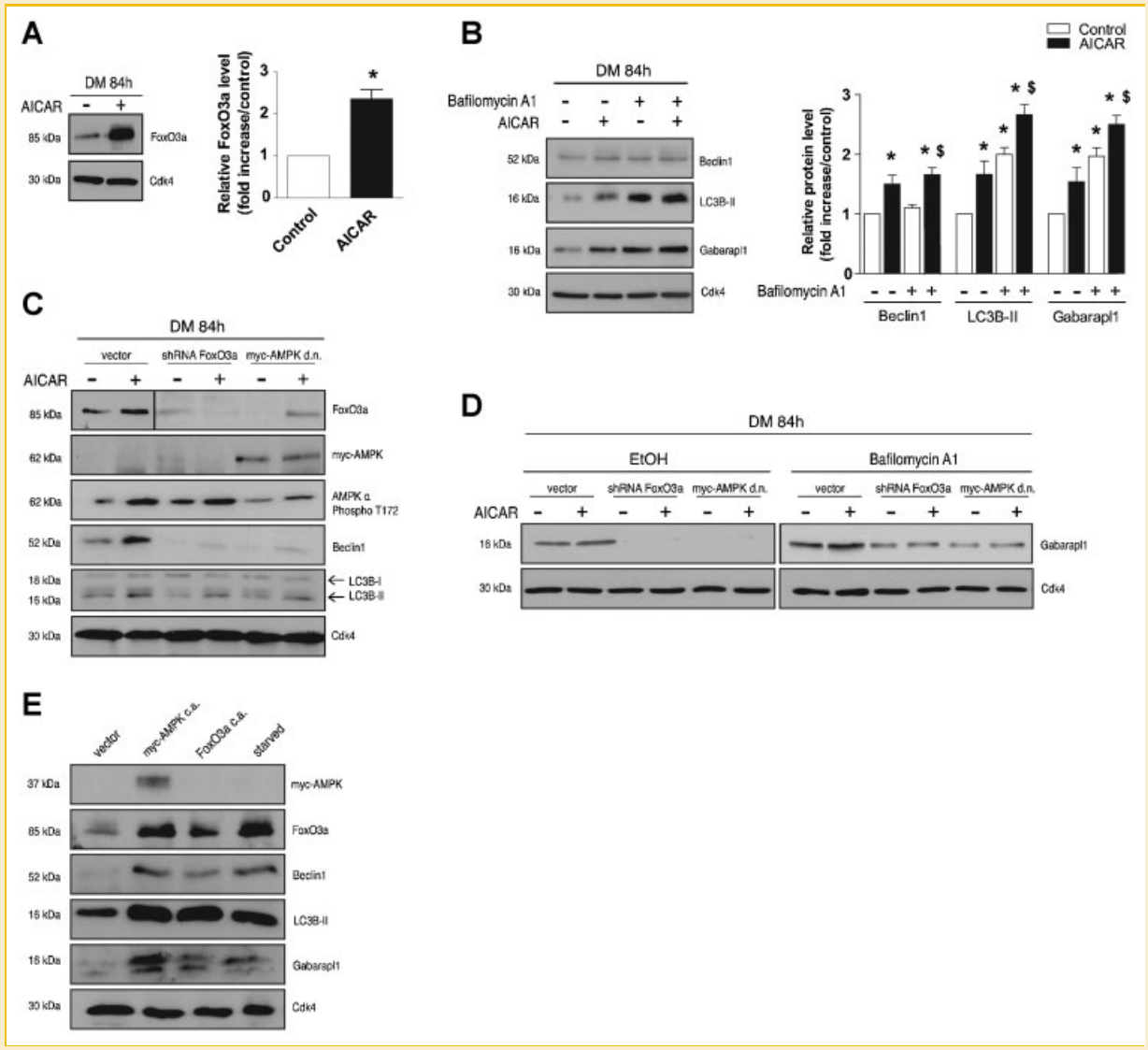

Fig. 3. AMPK activation leads to a FoxO3a-dependent Atg proteins increase in primary myotubes. A: Primary cultures of the mouse satellite cells were differentiated for 3 days and treated with 1 mM AICAR for additional 12 h in the same medium. Total lysates were analyzed by immunoblotting using anti-FoxO3a antibody. Cdk4 was used as a loading control. Quantification of FoxO3a expression in AICAR treated cells and control cells. Data displayed represent the mean and SEM of four independent experiments. $^{*}P < 0.01$ compared to control. B: Primary cultures of the mouse satellite cells were differentiated for 3 days and treated with 1 mM AICAR for additional 12 h in the same medium, in the presence or absence of Bafilomycin A1 (200 nM). Negative control cells (EtOH) were treated with the solvent ethanol. Total lysates were analyzed by immunoblotting using the indicated antibodies and phospho-specific antibodies. Cdk4 was used as a loading control. Quantification of LC3B-II, Beclin1, and Gabarapl1 protein expression in AICAR treated and control cells. Data displayed represent the mean and SEM of four independent experiments. $^{*}P < 0.01$ compared to control. $\$P < 0.01$ compared control + Bafilomycin A1. C: Mouse primary cultured satellite cells were transfected with FoxO3a shRNA plasmid or a plasmid encoding a dominant negative form of AMPK. Control cells were transfected with the corresponding core empty vector. Three days after differentiation, cells were incubated in differentiation medium containing 1 mM AICAR for 12 h and immunoblotting was performed on the total lysate. D: Mouse primary cultured satellite cells were transfected with FoxO3a shRNA plasmid or a plasmid encoding a dominant negative form of AMPK. Control cells were transfected with the corresponding core empty vector. Three days after differentiation, cells were incubated in differentiation medium containing 1 mM AICAR for additional 12 h in the presence or absence of Bafilomycin A1 (200 nM). Negative control cells (EtOH) were treated with the solvent ethanol. E: Adult Tibialis Anterior muscles were electroporated with either AMPK or FoxO3a mutated vectors. Negative muscle controls were transfected with the core vector of the constructs. Positive control corresponds to 2 days starved mice. Mice were sacrificed 14 days later. Muscle extracts were resolved onto SDS-PAGE. Specific antibodies were used as indicated for immunoblotting. Cdk4 was used as a loading control.

determined for each time point. Interestingly, analysis showed that FoxO3a accumulated in the nucleus from 30 min to 6 h during AICAR treatment and that FoxO3a increased in the cytosolic compartment from 6 to 24 h of treatment (Fig. 4A). We confirmed the absence of endogenous FoxO3a translocation from the cytoplasm to the nucleus at 24 h post-treatment (Fig. 4A).

Molecular interaction between FoxO3a and AMPK was analyzed in C2C12 myoblasts by co-immunoprecipitation of GFP-tagged

FoxO3a with endogenous AMPK and by co-immunoprecipitation of myc-tagged AMPK with endogenous FoxO3a. Results clearly indicated an association between the two proteins (Fig. 4B). Furthermore, AICAR treatment slightly increased the interaction between the two proteins (Fig. 4B).

AMPK INTERACTS WITH ULK1 AND WITH THE COMPONENTS OF mTORC1

Proteomics screens of the autophagy system have shown that AMPK may interact with components of the autophagy pathway [Behrends et al., 2010]. To test this interaction, a myc-tagged AMPK (WT) plasmid was transfected into C2C12 cells and proteins associated with autophagy including Ulk1, Beclin1, Gabarapl1, LC3, or Atg5 were then tested for co-immunoprecipitation. We observed that only endogenous Ulk1 interacted with AMPK; none of the other Atg proteins interacted with AMPK in our conditions (Fig. 5A). Myc-tagged Ulk1 plasmid was then transfected into C2C12 cells, which were then tested for co-immunoprecipitation with AMPK. Figure 5B clearly shows an association between the two proteins. Ulk1 is a serine–threonine-protein kinase also called Unc-51-like kinase 1 and plays a key role at the most upstream step like the initial stages of autophagy induction, the nucleation, and the formation of the pre-autophagosome structures [Mizushima et al., 1998]. The molecular association between AMPK and Ulk1 reported here confirms, and extends to muscle cells, the recent results obtained by Lee et al. [2010] suggesting that the regulation of Ulk1 by AMPK is crucial for the autophagy process.

Previous studies in HEK293T, HeLa, and MEFs cells have shown that mTORC1 inhibits autophagy by interacting with Ulk1 and its cofactors Atg13 or FIP200 [Jung et al., 2009]. Thus, we tested the existence of an interaction between mTORC1 components, AMPK and Ulk1/Atg13/FIP200 by co-immunoprecipitation. Our results

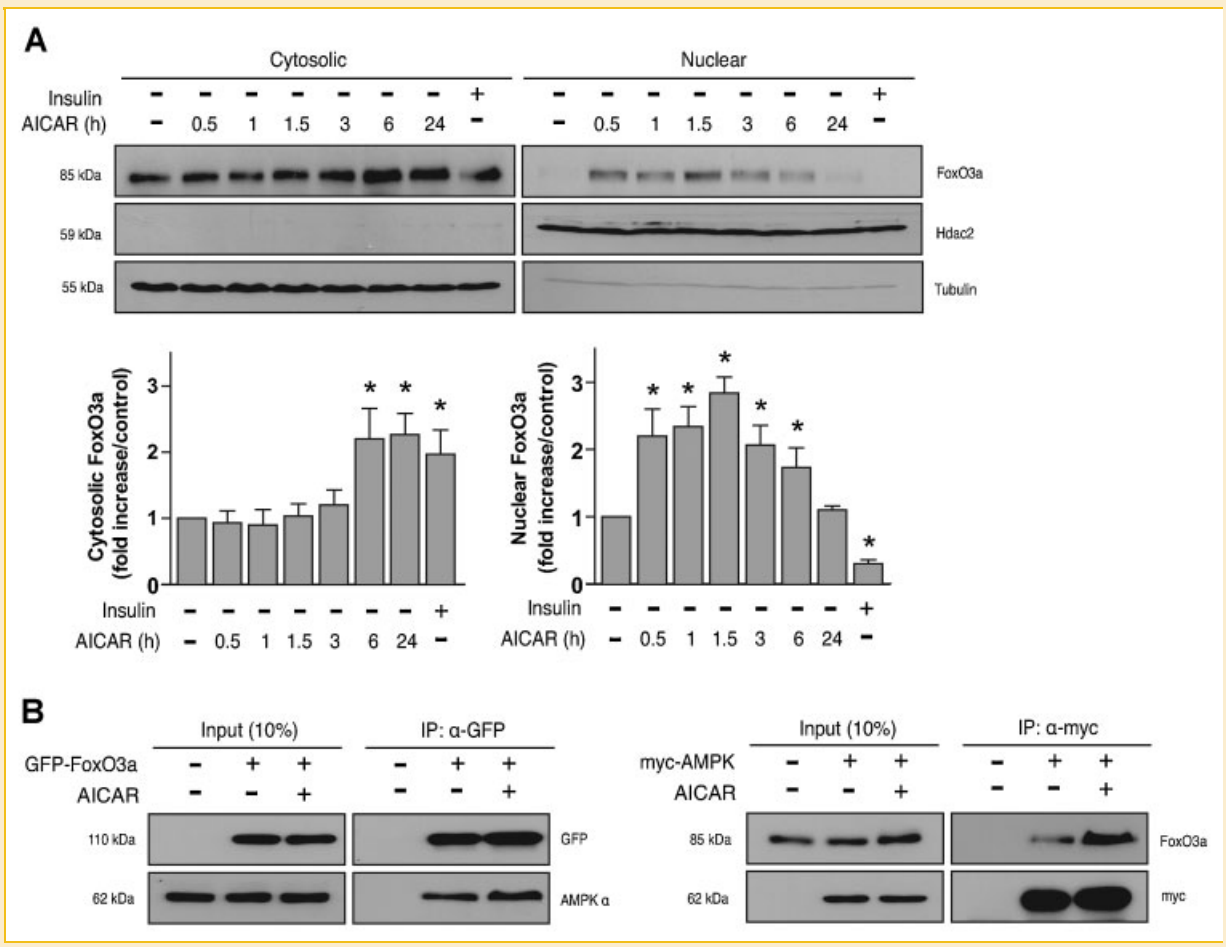

Fig. 4. AMPK induces a transient nuclear relocalization of FoxO3a in differentiated myotubes. A: Extraction of nuclear and cytosolic proteins from C2C12 myotube cultures treated with 1 mM AICAR for 0.5–1–1.5–3–6–24 h or insulin (1 h) were extracted. Samples were analyzed for nuclear and cytosolic FoxO3a, tubulin (cytosolic indicator), and Hdac2 (nuclear indicator) by immunoblotting. Data displayed represent the mean and SEM of five independent experiments. $^{*}P < 0.01$ compared to control. B: C2C12 cells were transfected with a plasmid encoding GFP-tagged FoxO3a WT or myc-tagged AMPK WT or the corresponding empty control plasmids. At 48 h after transfection, cells were treated with 1 mM AICAR for 3 h; cytosolic proteins were extracted for co-immunoprecipitation with anti-GFP and probed with anti-AMPK or with anti-myc and probed with anti-FoxO3a.

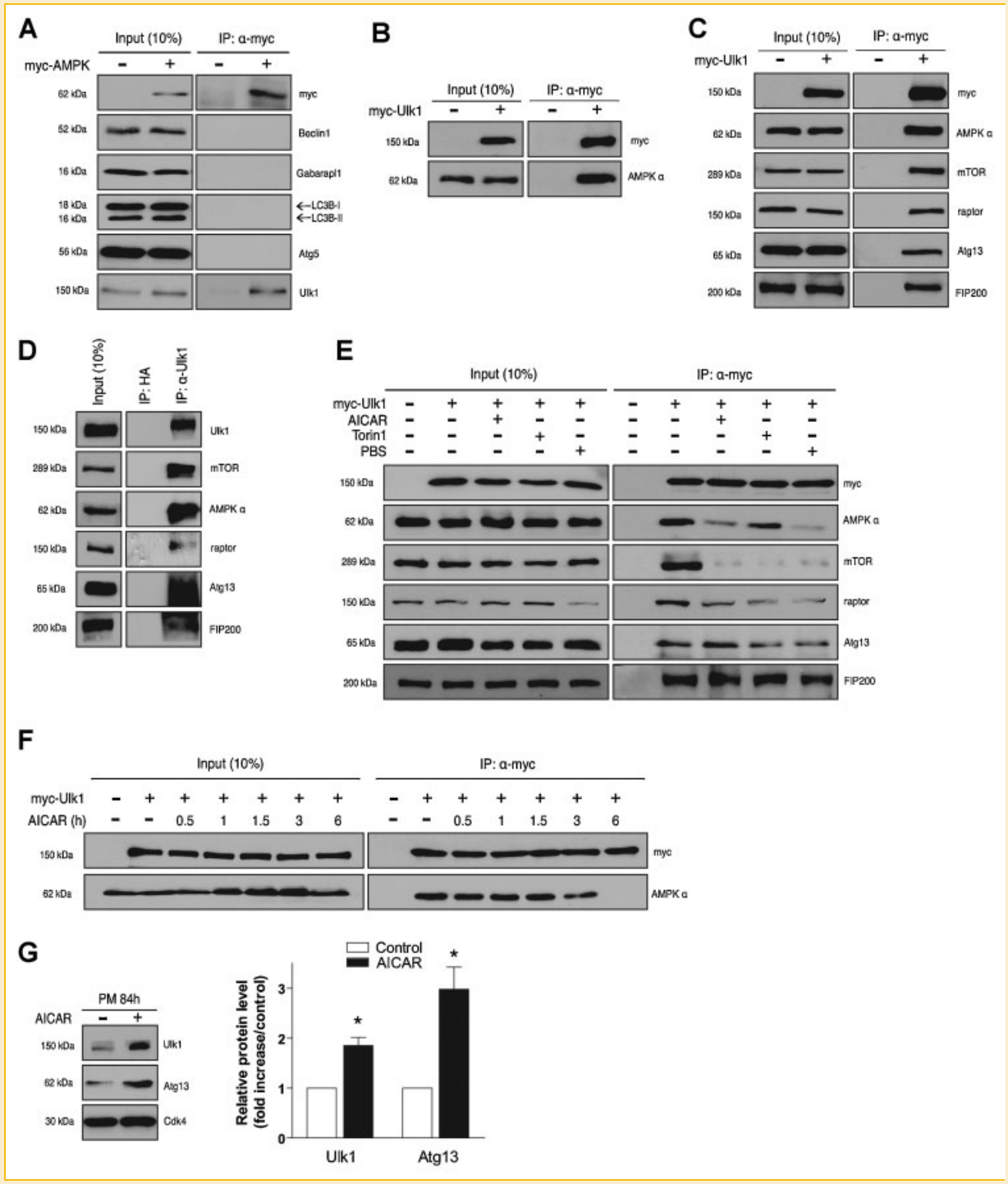

Fig. 5. AMPK interacts with the serine–threonine–protein kinase Ulk1. A: C2C12 cells were transfected with a plasmid encoding myc-tagged AMPK or an empty control plasmid. Forty eight hours after transfection, cytosolic proteins were extracted for co-immunoprecipitation with anti-myc and probed with anti -Beclin1, -Gabarapl1, -LC3, -Atg5, or -Ulk1. B: C2C12 cells were transfected with a plasmid encoding myc-tagged Ulk1 or an empty control plasmid. Forty eight hours after transfection, the cytosolic lysate was extracted for co-immunoprecipitation with anti-myc, followed by probing with anti-AMPK. C: C2C12 cells were transfected with a plasmid encoding myc-tagged Ulk1. At 48 h after transfection, the cytosolic lysate was extracted for co-immunoprecipitation with anti-myc, followed by probing with anti -AMPK, -mTOR, -raptor, -Atg13, or -FIP200. D: Endogenous Ulk1 was immunoprecipitated and assayed for association with mTOR/AMPK/raptor/Atg13/FIP200 by immunoblotting. Rabbit polyclonal antibody against HA tag was immunoprecipitated as control. E: C2C12 cells were transfected with a plasmid encoding myc-tagged Ulk1 or an empty control plasmid. At 48 h after transfection, cells were treated with 1 mM AICAR for 3 h, 250 nM Torin1 for 2 h or were starved by removal of growth medium, amino acids, and glucose and incubated in modified PBS for 3 h. Cytosolic proteins were extracted for co-immunoprecipitation with anti-myc and probed with anti -AMPK, -mTOR, -raptor, -Atg13, or -FIP200 antibodies. F: C2C12 cells were transfected with a plasmid encoding myc-tagged Ulk1. At 48 h after transfection, cells were treated at various times with 1 mM AICAR. Lysate was extracted for co-immunoprecipitation with anti-myc, followed by probing with anti-AMPK. G: C2C12 myoblasts were cultured in proliferation medium (PM) for 3 days and treated with 1 mM AICAR for additional 12 h. Immunoblotting was performed on total lysate to detect Ulk1 and Atg13. Cdk4 was used as a loading control. Error bars represent the mean and SEM of four independent experiments. $^{*}P < 0.01$ compared to control. These data are representative of at least three independent experiments.

reveal that mTOR/raptor proteins interact with the Ulk1/Atg13/FIP200 complex after immunoprecipitation with exogenous myc-tagged Ulk1 (Fig. 5C) or with endogenous Ulk1 (Fig. 5D).

Next, we investigated the binding efficiency of Ulk1, FIP200, Atg13, mTOR, Raptor in C2C12 myoblasts during autophagy induction. We found that Ulk1 associates with mTOR, Raptor, FIP200, and Atg13 prior to autophagy induction and that the stability of this complex is altered by activation of AMPK by AICAR (3 h), by starvation (3 h) or by administration of the mTOR inhibitor, Torin1 (2 h). Indeed, we reported that mTOR and Raptor proteins dissociate from the Ulk1-FIP200-Atg13 complex, whereas this complex is not altered by autophagy conditions (Fig. 5E).

Moreover, Ulk1-AMPK association was analyzed by co-immunoprecipitation with the same treatments as above. We reported that AMPK interacts with Ulk1 to form a complex in control cells and that autophagy-related treatments decrease Ulk1-AMPK interaction (Fig. 5E). In order to study the stability of this interaction during AICAR-induced autophagy, we carried out time course myc-Ulk1/AMPK co-immunoprecipitation experiments. We showed clearly that this complex starts to dissociate 3 h after activation of AMPK by AICAR and the dissociation is complete 6 h after autophagy induction (Fig. 5F).

In addition, although we observed that the Ulk1-FIP200-Atg13 complex is stable during AICAR treatment, the expression levels of Ulk1 and Atg13 were increased (Fig. 5G).

AMPK INDUCES THE PHOSPHORYLATION OF FoxO3a AND ULK1 IN MUSCLE CELLS

Our results showed clearly that AMPK interacts with FoxO3a and Ulk1. However, the type of interaction is not well documented in muscle cells. Greer et al. [2007] showed that AMPK directly regulates the mammalian FoxO3a transcription factor in 293 cells. Tong et al. [2009] reported, in C2C12 myoblasts, that AICAR treatment mediates skeletal muscle protein degradation through decrease of FoxO3a phosphorylation at Thr 318/321, two major sites known to be phosphorylated by Akt. Concerning the interaction AMPK/Ulk1, Lee et al. [2010] showed recently that AMPK is a new binding partner for Ulk1 in 293T cells. However, in muscle cells, the phosphorylation of these targets is not yet characterized. Amino-acid sequence analysis of Ulk1 reveals that Ser467 is a potential phosphorylation site (amphipathic helix; ø*X*ß*XX*(S/T)*XXX*ø, where ø represents a hydrophobic residue and ß represents a basic residue) [Dale et al., 1995; Weekes et al., 1993]. We analyzed in C2C12 cells whether the activation of AMPK by AICAR leads to the phosphorylation of this putative site. By immunoblotting, we found that AICAR treatment induced the phosphorylation of Ulk1 (2.3-fold increase) and FoxO3a (2.1-fold increase) at Ser467 and Ser588, respectively (Fig. 6B,C). Taken together, our results showed that AMPK interacts with FoxO3a and Ulk1 and induces their phosphorylation in C2C12 cells.

DISCUSSION

In the present work, we provided several important new insights concerning the implication of the energy sensor AMPK in muscle size control and, precisely, in the regulation of the autophagy program. We first clarified the molecular basis of the mode of regulation of FoxO3a-mediated autophagy by AMPK and, thereafter, we identified an interacting partner of AMPK directly implicated in autophagy initiation.

The FoxO subfamily of transcription factors integrates cellular signals emanating from growth factors, insulin, cytokines, and oxidative stress via a combination of post-translational modifications, including phosphorylation, acetylation, and ubiquitination [Brunet et al., 1999, Calnan and Brunet, 2008]. AMPK has been recently found to phosphorylate FoxO3a, but not FoxO1 or FoxO4 [Greer et al., 2007]. Although Akt phosphorylates FoxO3a on residues leading to its inhibition [Brunet et al., 1999], the phosphorylation of FoxO3a by AMPK on Ser588, triggered by stimuli that decrease cellular energy levels, leads to its activation [Greer et al., 2007]. In the first part of this article, we have demonstrated that AMPK regulates autophagy in a FoxO3a-dependent manner in C2C12 myoblasts and satellite cells. These data are in agreement and complete, recent findings of Romanello et al. [2010] showing that AMPK modulates FoxO3a RNA targets. Indeed, after AICAR treatments, authors showed that MAFbx, MuRF1, LC3, and Bnip3 mRNAs were upregulated without any change in Akt phosphorylation in C2C12 cells. Here, in mouse primary cultured satellite myotubes, we found an increase of MAFbx and MuRF1 protein level, whose expression is thought to be transcriptionally regulated by FoxO3a as shown by previous studies [Nakashima et al., 2008]. Interestingly, the strong accumulation of ubiquitined proteins reported in our study is consistent with an activation of the proteasomal-dependent proteolysis. Moreover, we confirmed an increase of the expression of Atgs proteins known to be regulated by FoxO3a after AMPK activation and extended this result to Atgs Ulk1 and Atg13. However, due to the fact that we were not able to completely block AMPK activity by the use of dominant negative AMPK, we cannot totally exclude some AMPK-independent FoxO3a activating effect of AICAR. Utilization of AMPK knockout mice will be necessary to address this point. Under basal conditions, a low level of autophagy is necessary to degrade and recycle long lived or toxic proteins and damaged organelles to maintain cell viability and cellular homeostasis [Nishida et al., 2008]. Our data present the molecular basis of a model in which, under conditions of energy stress leading to AMPK activation such as starvation or exercise, FoxO3a activity is regulated by AMPK to mobilize protein degradation as a source of alternative nutrient production and energy substrates. Overall, autophagy is required for normal cellular function and for response to multiple types of stress to maintain skeletal muscle function since skeletal muscle is constantly subjected to constraints requiring an important protein turnover. At any rate, it is unclear whether induction of autophagy is a compensatory mechanism to prevent a disease progression or a cause of pathophysiology. It is increasingly apparent that autophagy can have both beneficial and detrimental effects on muscle cells depending on the origin of its activation. Notably, we found that AMPK activation by AICAR treatment during 24 h leads to the poly (ADP-ribose) Polymerase (PARP) cleavage, an event known to lead to cell apoptosis (data not shown).

Moreover, we investigated the mechanisms of regulation of FoxO3a by AMPK. Although phosphorylation sites of FoxO3a by

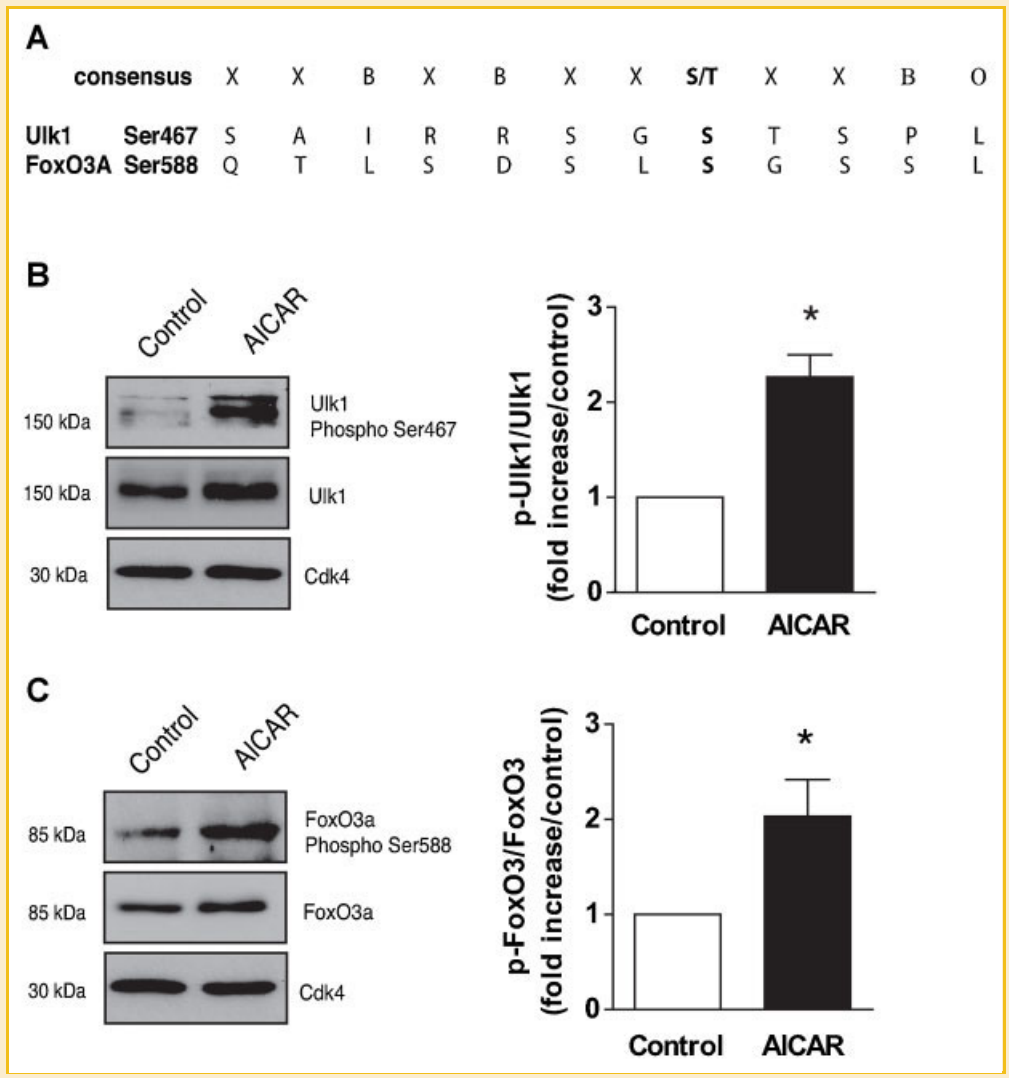

Fig. 6. AICAR induces phosphorylation of FoxO3a at Ser588 and Ulk1 at Ser467. A: Alignments of the AMPK consensus phosphorylation motif with putative phosphorylation sites in human FoxO3a and in human Ulk1. O, hydrophobic; B, basic. B: C2C12 myoblasts were cultured in proliferation medium for 3 days and treated with 1 mM AICAR for 3 h. Immunoblotting was performed on total lysate to detect Phospho-Ulk1 at Ser467. Cdk4 was used as a loading control. Error bars represent the mean and SEM of four independent experiments. $^{*}P < 0.01$ compared to control. C: C2C12 myoblasts were cultured in proliferation medium for 3 days and treated with 1 mM AICAR for 3 h. Immunoblotting was performed on total lysate to detect Phospho-FoxO3a at Ser588. Cdk4 was used as a loading control. Error bars represent the mean and SEM of four independent experiments. $^{*}P < 0.01$ compared to control.

AMPK had been identified [Greer et al., 2007], the type of regulation was not yet completely elucidated in muscle cells. Here we showed that the phosphorylation induced by AMPK on the residue Ser588 is conserved in muscle cells. A recent report showed that AICAR treatment on C2C12 myotubes leads to a decrease in nuclear FoxO3a level [Williamson et al., 2009]. In the present study, we failed to detect any variation in nuclear content of FoxO3a after AMPK activation for long treatments (i.e., 24 h) but we found an increase in the total protein level from 30 min. Interestingly, with short time course (30 min–6 h) the activation of AMPK by AICAR leads to a relocalization of FoxO3a in the nucleus, consistent with the results of Tong et al. [2009] who reported that AICAR treatment caused FoxO3a nuclear relocation due to a decrease in FoxO3a phosphorylation at Thr-318/321. However, Greer et al. [2007] have reported an increase of FoxO3a transcriptional activity without any change in the nuclear content of the factor after AMPK activation by 2-deoxy-glucose in HEK293T cells. Taken together, these divergent data strongly suggest that FoxO3a relocalization into the nucleus is not necessarily required to increase its transcriptional function and phosphorylation by AMPK may also control the FoxO3a protein stability. In agreement with this hypothesis, we reported here that negative dominant of AMPK leads to a critical decrease of FoxO3a protein level whereas AICAR treatment and constitutive active AMPK elicit an accumulation of the protein.

On the other hand, a study with FoxO1 showed that in addition to its transcriptional function, this factor interacts, after acetylation,

with Atgs and is required for the induction of autophagy [Zhao et al., 2010]. To test the existence of a similar relation with FoxO3a, we investigated the interaction of this factor with Beclin1, Ulk1, Atg13, Atg5, LC3, or Gabarapl1 after AICAR treatment. We did not detect any interaction between FoxO3a and these Atgs, suggesting in our model that the role of FoxO3a only resides in the transcription of these Atgs (data not shown).

In a second part of this study, we determined the connections between AMPK, the mTORC1 pathway, and autophagy. Firstly, we tested in mouse primary culture myotubes that activation of AMPK inhibits mTORC1. As reported in other cellular models [Wullschleger et al., 2006; Ma and Blenis, 2009], we found a decrease in mTORC1 pathway activity. In addition, we reported for the first time that the cap-dependent translation was inhibited by AMPK activation in primary myotubes. Interestingly, we also found that the insulin-induced activation of protein translation was totally inhibited when AMPK is phosphorylated, completing previous findings by Deshmukh et al. [2008] who have reported a total inhibition of the insulin-induced activation of mTORC1 in skeletal muscle with similar treatments. In addition, the inhibitory effect of AMPK activation on mTORC1 signaling was reported on a model of high frequency electrical stimulation of rat EDL muscle [Thomson et al., 2008].

We especially identified a multiprotein complex composed of AMPK, mTORC1, Ulk1, FIP200, and Atg13 in muscle cells. These data fit with the model found in other cell types showing that, under basal conditions, mTORC1 interacts with Ulk1 and prevents autophagy, in opposition to energy stress conditions [Hosokawa et al., 2009a]. Under nutrient-rich conditions, repressive phosphorylation of Ulk1 by mTORC1 modulates Ulk1 kinase activity and/or its ability to interact with the cofactors Atg13 or FIP200, thereby it coordinates the autophagy response [Ganley et al., 2009; Hara and Mizushima, 2009]. For the first time we report in muscle cells that activation of AMPK by AICAR or inhibition of mTORC1 with either Torin1 or amino acid starvation removes AMPK and mTOR/raptor from the Ulk1 complex, a process that may initiate the Ulk1-dependent phosphorylation of Atg13 and FIP200 leading to the activation of autophagy [Jung et al., 2009]. More precisely, the association of FIP200 with Ulk1 is Atg13-dependent and this interaction controls Ulk1 turnover [Ganley et al., 2009; Hara and Mizushima, 2009].

Results obtained by several groups on HEK293T and MEF cells have shown that induction of autophagy by amino acid starvation or Rapamycin treatment failed to significantly alter the affinity of the interaction between Ulk1, FIP200, and Atg13 [Hara et al., 2008; Ganley et al., 2009; Jung et al., 2009; Hosokawa et al., 2009b]. Our results extend to muscle cells the fact that Ulk1, FIP200, and Atg13 proteins interact prior to autophagy induction to form a complex which remains stable after activation of AMPK by AICAR or inhibition of mTORC1 with either Torin1 or amino acid privation. Noteworthy, increase of the starvation time to 6 h, AICAR treatment to 12 h, and 250 nM Torin1 treatment to 3 h leads to an instability of the Ulk1-FIP200-Atg13 complex (data not shown). This effect could be explained in part by an apoptotic response linked to Ulk1 overexpression, prolonged AMPK activation, or prolonged starvation [Martinet et al., 2005; Scott et al., 2007; Hara et al., 2008; Williamson et al., 2009]. However, we cannot exclude that in C2C12 myoblasts, unlike HEK293T and MEF cells, Ulk1-FIP200-Atg13 complex dissociates during autophagy process. This mechanism could be implicated in the regulation of autophagy termination. Additional experiments will be necessary to address this issue.

Proteomics screens of the autophagy system [Behrends et al., 2010] and a co-immunoprecipitation study performed in HEK293T cells [Lee et al., 2010] have shown that AMPK may interact with Ulk1 and Ulk2. Here, we clearly demonstrated that AMPK is required for muscle autophagy and interacts with Ulk1. Given our data, we suggest a model in which the multiprotein Ulk1 complex possesses binding sites for AMPK, mTOR/raptor, Atg13, and FIP200. During the submission of this manuscript, in two additional studies it was demonstrated that Ulk1 is phosphorylated by AMPK in HEK293 cells [Egan et al., 2011; Kim et al., 2011]. We reported in muscle cells that the Ser467 site identified by Egan et al. is phosphorylated by AMPK. This event could participate to a conformational change and thus disrupts the interaction between Ulk1 and mTORC1, in agreement with the suppression of mTORC1 anti-autophagy activity in the Ulk1 complex [Hosokawa et al., 2009a]. In addition, Ulk1 phosphorylation by AMPK may directly activate Ulk1 kinase activity. Indeed, it was shown in vitro that Ulk1 is highly phosphorylated and that purified Ulk1 can phosphorylate itself and requires autophosphorylation for stability [Dorsey et al., 2009].

Interestingly, we found that following autophagy induction, AMPK started to dissociate from Ulk1 3 h after AICAR treatment and dissociation is complete after 6 h. In agreement with our results, Wang's group reported, in Hela cells, that AMPK is associated with Ulk1 only under nutrient-rich condition and dissociated from Ulk1 after starvation [Shang et al., 2011]. However, this process is faster than in muscle cells since AMPK started to dissociate from Ulk1 5 min after starvation. Thus, in the light of these results, we can suggest that in normal condition Ulk1 is associated to AMPK, upon AICAR-induced autophagy the complex remains stable for 3 h and afterwards start to dissociate. As suggested by Shang et al., we can propose that Ulk1 dissociates from AMPK and thus becomes more active, or conversely, that AMPK-Ulk1 dissociation is responsible for a negative regulatory feedback loop. Recently, Loffler et al. [2011] showed that Ulk1-mediated phosphorylation of AMPK constitutes an inhibitory feedback control. Further work will be needed to define the molecular mechanisms for these autophagy-induced events.

According to our finding, it is now evident that AMPK activates protein degradation in muscle cells by regulating autophagy through two major signaling pathways (Fig. 7). The first one involves FoxO3a activation by AMPK leading to an increase in Atgs expression, which acts as a promoter of the autophagosome formation. The second one involves a post-translational regulation of the mTORC1/Ulk1/Atg13/FIP200 complex by AMPK playing a critical role in the initiation of the autophagy pathway. The identification of Ulk1 as a direct target of AMPK represents a significant step towards the understanding how cellular energy stress regulates autophagy machinery in muscle cells. Further studies directed at identifying the molecular basis of these phenomena will be essential to understand how Ulk1 activation results in initiation of the autophagy pathway. Based on these data it

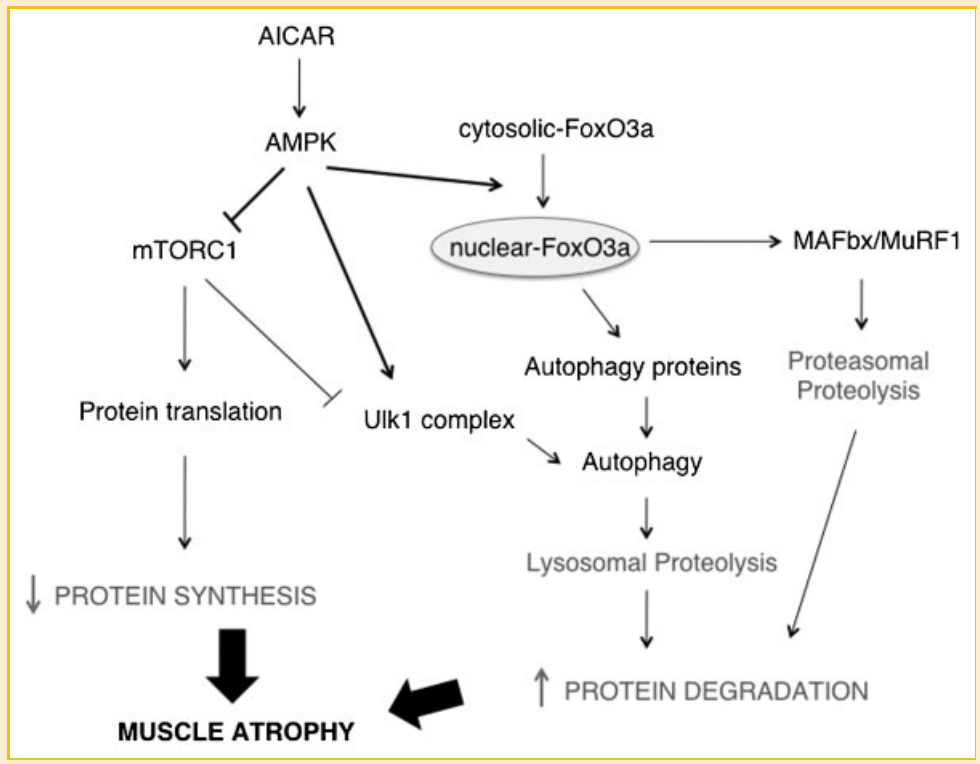

Fig. 7. Schematic of mechanisms regulating atrophy of skeletal muscle downstream of AMPK.

is clearly conceivable that the AMPK/autophagy system must be considered not only in muscle homeostasis but also in muscle pathologies such as sarcopenia and myopathies.

ACKNOWLEDGMENTS

The authors thank Dr. A. Brunet (Stanford University, CA) for the generous gift of the phospho-Ser588 FoxO3a antibody and her precious help for the study. They thank Drs. D. Carling (Imperial College London), P. Storz (Mayo Clinic, Jacksonville, FL), and J. Blenis (Harvard Medical School, Boston) for the gift of plasmids. They thank the Whitehead institute and the DFCI for supplying Torin1 inhibitor. The authors are grateful to Drs A. Bonnieu, B. Chabi, S.A. Leibovitch, V. Ollendorff, and L. Tintignac for their helpful discussion. This work was supported by a fellowship from the Ministère de la Recherche et de la Technologie (to AMJS).

REFERENCES

Anderson MJ, Viars CS, Czekay S, Cavenee WK, Arden KC. 1998. Cloning and characterization of three human forkhead genes that comprise an FKHR-like gene subfamily. Genomics 47(2):187–199.

Behrends C, Sowa ME, Gygi SP, Harper JW. 2010. Network organization of the human autophagy system. Nature 466(7302):68–76.

Beugnet A, Tee AR, Taylor PM, Proud CG. 2003. Regulation of targets of mTOR (mammalian target of rapamycin) signalling by intracellular amino acid availability. Biochem J 372(Pt 2):555–566.

Bodine SC, Latres E, Baumhueter S, Lai VK, Nunez L, Clarke BA, Poueymirou WT, Panaro FJ, Na E, Dharmarajan K, Pan ZQ, Valenzuela DM, DeChiara TM, Stitt TN, Yancopoulos GD, Glass DJ. 2001a. Identification of ubiquitin ligases required for skeletal muscle atrophy. Science 294(5547):1704–1708.

Bodine SC, Stitt TN, Gonzalez M, Kline WO, Stover GL, Bauerlein R, Zlotchenko E, Scrimgeour A, Lawrence JC, Glass DJ, Yancopoulos GD. 2001b. Akt/mTOR pathway is a crucial regulator of skeletal muscle hypertrophy and can prevent muscle atrophy in vivo. Nat Cell Biol 3(11):1014–1019.

Brunet A, Bonni A, Zigmond MJ, Lin MZ, Juo P, Hu LS, Anderson MJ, Arden KC, Blenis J, Greenberg ME. 1999. Akt promotes cell survival by phosphorylating and inhibiting a Forkhead transcription factor. Cell 96(6):857–868.

Calnan DR, Brunet A. 2008. The FoxO code. Oncogene 27(16):2276–2288.

Castro MJ, Apple DF Jr, Staron RS, Campos GE, Dudley GA. 1999. Influence of complete spinal cord injury on skeletal muscle within 6 mo of injury. J Appl Physiol 86(1):350–358.

Codogno P, Meijer AJ. 2005. Autophagy and signaling: their role in cell survival and cell death. Cell Death Differ 12(Suppl 2):1509–1518.

Csibi A, Cornille K, Leibovitch MP, Poupon A, Tintignac LA, Sanchez AM, Leibovitch SA. 2010. The translation regulatory subunit eIF3f controls the kinase-dependent mTOR signaling required for muscle differentiation and hypertrophy in mouse. PLoS One 5(2):e8994.

Dale S, Wilson WA, Edelman AM, Hardie DG. 1995. Similar substrate recognition motifs for mammalian AMP-activated protein kinase, higher plant HMG-CoA reductase kinase-A, yeast SNF1, and mammalian calmodulin-dependent protein kinase I. FEBS Lett 361(2–3):191–195.

Derave W, Ai H, Ihlemann J, Witters LA, Kristiansen S, Richter EA, Ploug T. 2000. Dissociation of AMP-activated protein kinase activation and glucose transport in contracting slow-twitch muscle. Diabetes 49(8):1281–1287.

Deshmukh AS, Treebak JT, Long YC, Viollet B, Wojtaszewski JF, Zierath JR. 2008. Role of adenosine 5'-monophosphate-activated protein kinase subunits in skeletal muscle mammalian target of rapamycin signaling. Mol Endocrinol 22(5):1105–1112.

Dorsey FC, Rose KL, Coenen S, Prater SM, Cavett V, Cleveland JL, Caldwell-Busby J. 2009. Mapping the phosphorylation sites of Ulk1. J Proteome Res 8(11):5253–5263.

Egan DF, Shackelford DB, Mihaylova MM, Gelino S, Kohnz RA, Mair W, Vasquez DS, Joshi A, Gwinn DM, Taylor R, Asara JM, Fitzpatrick J, Dillin A, Viollet B, Kundu M, Hansen M, Shaw RJ. 2011. Phosphorylation of ULK1 (hATG1) by AMP-activated protein kinase connects energy sensing to mitophagy. Science 331(6016):456–461.

Fitts RH, Riley DR, Widrick JJ. 2001. Functional and structural adaptations of skeletal muscle to microgravity. J Exp Biol 204(Pt 18):3201–3208.

Ganley IG, Lam du H, Wang J, Ding X, Chen S, Jiang X. 2009. ULK1.-ATG13.FIP200 complex mediates mTOR signaling and is essential for autophagy. J Biol Chem 284(18):12297–12305.

Gomes MD, Lecker SH, Jagoe RT, Navon A, Goldberg AL. 2001. Atrogin-1, a muscle-specific F-box protein highly expressed during muscle atrophy. Proc Natl Acad Sci USA 98(25):14440–14445.

Greer EL, Oskoui PR, Banko MR, Maniar JM, Gygi MP, Gygi SP, Brunet A. 2007. The energy sensor AMP-activated protein kinase directly regulates the mammalian FOXO3 transcription factor. J Biol Chem 282(41):30107–30119.

Hara T, Mizushima N. 2009. Role of ULK-FIP200 complex in mammalian autophagy: FIP200, a counterpart of yeast Atg17? Autophagy 5(1):85–87.

Hara T, Takamura A, Kishi C, Iemura S, Natsume T, Guan JL, Mizushima N. 2008. FIP200, a ULK-interacting protein, is required for autophagosome formation in mammalian cells. J Cell Biol 181(3):497–510.

Hardie DG. 2007. AMP-activated/SNF1 protein kinases: Conserved guardians of cellular energy. Nat Rev Mol Cell Biol 8(10):774–785.

Hosokawa N, Hara T, Kaizuka T, Kishi C, Takamura A, Miura Y, Iemura S, Natsume T, Takehana K, Yamada N, Guan JL, Oshiro N, Mizushima N. 2009a. Nutrient-dependent mTORC1 association with the ULK1-Atg13-FIP200 complex required for autophagy. Mol Biol Cell 20(7):1981–1991.

Hosokawa N, Sasaki T, Iemura S, Natsume T, Hara T, Mizushima N. 2009b. Atg101, a novel mammalian autophagy protein interacting with Atg13. Autophagy 5(7):973–979.

Inoki K, Zhu T, Guan KL. 2003. TSC2 mediates cellular energy response to control cell growth and survival. Cell 115(5):577–590.

Jackman RW, Kandarian SC. 2004. The molecular basis of skeletal muscle atrophy. Am J Physiol Cell Physiol 287(4):C834–C843.

Jagoe RT, Goldberg AL. 2001. What do we really know about the ubiquitin-proteasome pathway in muscle atrophy? Curr Opin Clin Nutr Metab Care 4(3):183–190.

Jung CH, Jun CB, Ro SH, Kim YM, Otto NM, Cao J, Kundu M, Kim DH. 2009. ULK-Atg13-FIP200 complexes mediate mTOR signaling to the autophagy machinery. Mol Biol Cell 20(7):1992–2003.

Kabeya Y, Mizushima N, Ueno T, Yamamoto A, Kirisako T, Noda T, Kominami E, Ohsumi Y, Yoshimori T. 2000. LC3, a mammalian homologue of yeast Apg8p, is localized in autophagosome membranes after processing. EMBO J 19(21):5720–5728.

Kamei Y, Miura S, Suzuki M, Kai Y, Mizukami J, Taniguchi T, Mochida K, Hata T, Matsuda J, Aburatani H, Nishino I, Ezaki O. 2004. Skeletal muscle FOXO1 (FKHR) transgenic mice have less skeletal muscle mass, down-regulated Type I (slow twitch/red muscle) fiber genes, and impaired glycemic control. J Biol Chem 279(39):41114–41123.

Kim J, Kundu M, Viollet B, Guan KL. 2011. AMPK and mTOR regulate autophagy through direct phosphorylation of Ulk1. Nat Cell Biol 13(2):132–141.

Lecker SH, Jagoe RT, Gilbert A, Gomes M, Baracos V, Bailey J, Price SR, Mitch WE, Goldberg AL. 2004. Multiple types of skeletal muscle atrophy involve a common program of changes in gene expression. FASEB J 18(1):39–51.

Lee JW, Park S, Takahashi Y, Wang HG. 2010. The association of AMPK with ULK1 regulates autophagy. PLoS One 5(11):e15394.

Loffler AS, Alers S, Dieterle AM, Keppeler H, Franz-Wachtel M, Kundu M, Campbell DG, Wesselborg S, Alessi DR, Stork B. 2011. Ulk1-mediated phosphorylation of AMPK constitutes a negative regulatory feedback loop. Autophagy 7(7):696–706.

Ma XM, Blenis J. 2009. Molecular mechanisms of mTOR-mediated translational control. Nat Rev Mol Cell Biol 10(5):307–318.

Mammucari C, Milan G, Romanello V, Masiero E, Rudolf R, Del Piccolo P, Burden SJ, Di Lisi R, Sandri C, Zhao J, Goldberg AL, Schiaffino S, Sandri M. 2007. FoxO3 controls autophagy in skeletal muscle in vivo. Cell Metab 6(6):458–471.

Martinet W, De Meyer GR, Herman AG, Kockx MM. 2005. Amino acid deprivation induces both apoptosis and autophagy in murine C2C12 muscle cells. Biotechnol Lett 27(16):1157–1163.

Meijer AJ, Codogno P. 2004. Regulation and role of autophagy in mammalian cells. Int J Biochem Cell Biol 36(12):2445–2462.

Mitch WE, Goldberg AL. 1996. Mechanisms of muscle wasting. The role of the ubiquitin-proteasome pathway. N Engl J Med 335(25):1897–1905.

Mizushima N, Noda T, Yoshimori T, Tanaka Y, Ishii T, George MD, Klionsky DJ, Ohsumi M, Ohsumi Y. 1998. A protein conjugation system essential for autophagy. Nature 395(6700):395–398.

Mizushima N, Yamamoto A, Matsui M, Yoshimori T, Ohsumi Y. 2004. In vivo analysis of autophagy in response to nutrient starvation using transgenic mice expressing a fluorescent autophagosome marker. Mol Biol Cell 15(3): 1101–1111.

Nader GA, Hornberger TA, Esser KA. 2002. Translational control: Implications for skeletal muscle hypertrophy. Clin Orthop Related Res 403 (Suppl): S178–S187.

Nakashima K, Yakabe Y. 2007. AMPK activation stimulates myofibrillar protein degradation and expression of atrophy-related ubiquitin ligases by increasing FOXO transcription factors in C2C12 myotubes. Biosci Biotechnol Biochem 71(7):1650–1656.

Nakashima K, Yakabe Y, Ishida A, Katsumata M. 2008. Effects of orally administered glycine on myofibrillar proteolysis and expression of proteolytic-related genes of skeletal muscle in chicks. Amino Acids 35(2):451–456.

Nishida K, Yamaguchi O, Otsu K. 2008. Crosstalk between autophagy and apoptosis in heart disease. Circ Res 103(4):343–351.

Romanello V, Guadagnin E, Gomes L, Roder I, Sandri C, Petersen Y, Milan G, Masiero E, Del Piccolo P, Foretz M, Scorrano L, Rudolf R, Sandri M. 2010. Mitochondrial fission and remodelling contributes to muscle atrophy. EMBO J 29(10):1774–1785.

Rommel C, Bodine SC, Clarke BA, Rossman R, Nunez L, Stitt TN, Yancopoulos GD, Glass DJ. 2001. Mediation of IGF-1-induced skeletal myotube hypertrophy by PI(3)K/Akt/mTOR and PI(3)K/Akt/GSK3 pathways. Nat Cell Biol 3(11):1009–1013.

Salt IP, Connell JM, Gould GW. 2000. 5-aminoimidazole-4-carboxamide ribonucleoside (AICAR) inhibits insulin-stimulated glucose transport in 3T3-L1 adipocytes. Diabetes 49(10):1649–1656.

Sandri M, Sandri C, Gilbert A, Skurk C, Calabria E, Picard A, Walsh K, Schiaffino S, Lecker SH, Goldberg AL. 2004. Foxo transcription factors induce the atrophy-related ubiquitin ligase atrogin-1 and cause skeletal muscle atrophy. Cell 117(3):399–412.

Scott RC, Juhasz G, Neufeld TP. 2007. Direct induction of autophagy by Atg1 inhibits cell growth and induces apoptotic cell death. Curr Biol 17(1):1–11.

Shang L, Chen S, Du F, Li S, Zhao L, Wang X. 2011. Nutrient starvation elicits an acute autophagic response mediated by Ulk1 dephosphorylation and its subsequent dissociation from AMPK. Proc Natl Acad Sci USA 108(12):4788–4793.

Tanida I, Wakabayashi M, Kanematsu T, Minematsu-Ikeguchi N, Sou YS, Hirata M, Ueno T, Kominami E. 2006. Lysosomal turnover of GABARAP-phospholipid conjugate is activated during differentiation of C2C12cells to

myotubes without inactivation of the mTor kinase-signaling pathway. Autophagy 2(4):264–271.

Thomson DM, Fick CA, Gordon SE. 2008. AMPK activation attenuates S6K1, 4E-BP1, and eEF2 signaling responses to high-frequency electrically stimulated skeletal muscle contractions. J Appl Physiol 104(3):625–632.

Thoreen CC, Kang SA, Chang JW, Liu Q, Zhang J, Gao Y, Reichling LJ, Sim T, Sabatini DM, Gray NS. 2009. An ATP-competitive mammalian target of rapamycin inhibitor reveals rapamycin-resistant functions of mTORC1. J Biol Chem 284(12):8023–8032.

Tong JF, Yan X, Zhu MJ, Du M. 2009. AMP-activated protein kinase enhances the expression of muscle-specific ubiquitin ligases despite its activation of IGF-1/Akt signaling in C2C12 myotubes. J Cell Biochem 108(2):458–468.

Vavvas D, Apazidis A, Saha AK, Gamble J, Patel A, Kemp BE, Witters LA, Ruderman NB. 1997. Contraction-induced changes in acetyl-CoA carboxylase and 5'-AMP-activated kinase in skeletal muscle. J Biol Chem 272(20): 13255–13261.

Weekes J, Ball KL, Caudwell FB, Hardie DG. 1993. Specificity determinants for the AMP-activated protein kinase and its plant homologue analysed using synthetic peptides. FEBS Lett 334(3):335–339.

Williamson DL, Butler DC, Alway SE. 2009. AMPK inhibits myoblast differentiation through a PGC-1alpha-dependent mechanism. Am J Physiol Endocrinol Metab 297(2):E304–E314.

Wojtaszewski JF, Nielsen P, Hansen BF, Richter EA, Kiens B. 2000. Isoform-specific and exercise intensity-dependent activation of 5'-AMP-activated protein kinase in human skeletal muscle. J Physiol 528(Pt 1):221–226.

Woods A, Azzout-Marniche D, Foretz M, Stein SC, Lemarchand P, Ferre P, Foufelle F, Carling D. 2000. Characterization of the role of AMP-activated protein kinase in the regulation of glucose-activated gene expression using constitutively active and dominant negative forms of the kinase. Mol Cell Biol 20(18):6704–6711.

Wullschleger S, Loewith R, Hall MN. 2006. TOR signaling in growth and metabolism. Cell 124(3):471–484.

Xie Z, Nair U, Klionsky DJ. 2008. Atg8 controls phagophore expansion during autophagosome formation. Mol Biol Cell 19(8):3290–3298.

Yang YP, Liang ZQ, Gu ZL, Qin ZH. 2005. Molecular mechanism and regulation of autophagy. Acta Pharmacol Sin 26(12):1421–1434.

Zhao J, Brault JJ, Schild A, Cao P, Sandri M, Schiaffino S, Lecker SH, Goldberg AL. 2007. FoxO3 coordinately activates protein degradation by the autophagic/lysosomal and proteasomal pathways in atrophying muscle cells. Cell Metab 6(6):472–483.

Zhao Y, Yang J, Liao W, Liu X, Zhang H, Wang S, Wang D, Feng J, Yu L, Zhu WG. 2010. Cytosolic FoxO1 is essential for the induction of autophagy and tumour suppressor activity. Nat Cell Biol 12(7):665–675.